A study of the predictability of a 28-variable atmospheric model

By EDWARD N. LORENZ, *Det Norske Meteorologiske Institutt*[1,2]

(Manuscript received December 22; revised version February 1)

ABSTRACT

A 28-variable model of the atmosphere is constructed by expanding the equations of a two-level geostrophic model in truncated double-Fourier series. The model includes the nonlinear interactions among disturbances of three different wave lengths. Nonperiodic time-dependent solutions are determined by numerical integration.

By comparing separate solutions with slightly different initial conditions, the growth rate of small initial errors is studied. The time required for errors comparable to observational errors in the atmosphere to grow to intolerable errors is strongly dependent upon the current circulation pattern, and varies from a few days to a few weeks.

Some statistical predictability of certain quantities seems to be present even after errors in the complete circulation pattern are no longer small.

The feasibility of performing similar studies with much larger atmospheric models is considered.

1. Introduction

Among the many problems to which meteorologists have devoted their efforts over the past century, weather forecasting has continued to occupy a prominent position. Yet despite frequent improvements in the network of observing stations and advances in the technique of forecasting, weather predictions still do not enjoy the accuracy which many persons believe they have a right to expect. Comparisons are frequently made with predictions of such other natural phenomena as ocean tides and solar eclipses.

In contrast to the tides, which can be predicted about as accurately several years in advance as several days in advance, the precision with which we have thus far been able to predict the weather is closely related to the range of prediction—the amount of time in advance for which the prediction is made. Failure to produce perfect weather forecasts at any range of prediction must be ascribable to one or more of three general causes:

1. The atmospheric system is not determin-

istic; the present and past states of the atmosphere and its environment do not uniquely determine the state at all future times.

2. Observations are insufficient: regardless of whether the atmospheric system is deterministic, the observed present and past states of those portions of the atmosphere and its environment which are observed do not uniquely determine the future states.

3. Forecasting procedures are inadequate; presently used techniques do not duplicate the behavior of the atmosphere and its environment.

Concerning the first possible cause, one can easily present a case for the non-determinism of weather. Among other things, the atmosphere is affected at least to some extent by human activity, particularly when that activity takes the form of building large artificial lakes or removing vast forests. Any claim that the atmosphere is deterministic is therefore tantamount to a claim that human behavior is deterministic. It appears quite likely, however, that lack of determinism is not a significant contributing cause to our present failures in forecasting, in view of the remaining possible causes.

Concerning the second cause, it is evident that, regardless of the accuracy of our observing

instruments, many features remain unobserved simply because observations cannot be made everywhere. Even over populated land areas, thunderstorms may be lost between observing stations. Over parts of the ocean, entire tropical hurricanes may go unnoticed. Some of the effects of an incomplete knowledge of the present state of the atmosphere have been examined by THOMPSON (1957). More recently, the writer (1963a) has shown that if a system is varying nonperiodically, or with a nonperiodic component, and if in addition the present state or the present and past states are not known with complete accuracy, any forecasting procedure will lead to poorer and poorer forecasts as the range of prediction increases, until ultimately only the periodic component can be predicted in the far distant future. Herein lies a crucial difference between the tides, which are essentially periodic, and the weather, which is largely nonperiodic.

Concerning the third cause, it is obvious that forecasting procedures have yet to reach their ultimate state of perfection. It is common experience that under subjective procedures different forecasters make considerably different forecasts in the 'same situation. Obviously not all of these forecasts can be correct. Objective procedures include some which are primarily empirical and some which are based largely upon atmospheric dynamics. Empirical procedures have been confined for the most part to linear formulas, although the physical laws indicate that the optimum formulas are nonlinear. Dynamical procedures currently in routine use generally neglect the thermodynamic and radiative properties of water vapor and clouds, and do not adequately represent the effects of small-scale motions.

We do not really know whether improvements in forecasting methods would significantly alter the quality of forthcoming forecasts, in view of the limitations imposed by the current inadequacy of the observations. Likewise, we cannot state with certainty that improvement of our observational network would measurably improve our forecasts, in view of the deficiencies in forecasting procedures. It does seem virtually certain, however, that more refined forecasting techniques together with more widespread observations can lead to forecasts of a higher quality.

In this study we shall be concerned with the limitations upon forecast accuracy imposed by the second enumerated cause—the incompleteness and inaccuracy of observations. We shall be particularly interested in the minimum range of prediction for which typical errors in observing the present state lead to unacceptably poor forecasts. This range is not revealed by the theoretical studies previously mentioned—conceivably it could be a few days or a few years.

A currently popular method of studying the general circulation of the atmosphere consists of establishing closed systems of equations which to a certain extent approximate the equations governing the atmosphere and its environment, and then determining explicit time-dependent solutions of these equations by numerical integration. The systems of equations are viewed as mathematical models of the atmosphere, and the numerical solutions are treated as samples of observational data for the behavior of the models. Quantities which have been evaluated from real atmospheric data, e.g., horizontal fluxes of heat and momentum, may also be computed from a model, and a comparison of the values in the model with those in the atmosphere may give some indication of the adequacy of the model. Quantities which are not so readily evaluated from atmospheric data, e.g., vertical fluxes of heat and momentum, may likewise be computed from a model, and these computed values may serve as estimates of the corresponding atmospheric values.

The original numerical model of the general circulation was that of PHILLIPS (1956). In this model the three-dimensional atmosphere was replaced by two two-dimensional layers, and the horizontal structure of each layer was represented by a network of 272 points. The governing equations were those of a dry atmosphere in approximate hydrostatic and geostrophic equilibrium. Phillips obtained rates of generation, conversion, and dissipation of various forms of energy which were in qualitative and fair quantitative agreement with the rates prevailing in the real atmosphere.

More recent numerical models have departed from the prototype in two directions. Some investigators have attempted to make the structure of their models more like that of the atmosphere, by introducing more degrees of freedom in the vertical and horizontal directions, dropping the geostrophic constraint, and in-

cluding some of the effects of water vapor. Typical of the large models is a primitive-equation model of SMAGORINSKY (1963), where there are effectively four dependent variables at each of 1296 grid points.

Other investigators have attempted to reduce the number of degrees of freedom as far as possible, while still maintaining some resemblance between the behavior of the model and that of the atmosphere. The writer (1962), for example, has studied a twelve-variable model in which cyclones and anticyclones can move and change their configuration in a nonperiodic fashion. To achieve this simplification, it was necessary to restrict the fields of motion and temperature to a sinusoidal variation in the longitudinal direction, with a single prespecified wave length.

In the real atmosphere the fields of motion and temperature do not vary in a simple sinusoidal fashion, but each field may be expressed through harmonic analysis as a sum of sinusoidally varying component fields, plus a residual field which is independent of longitude. Among the interesting features of real atmospheric behavior are the interactions between different components; each component field of motion acts to distort each component field of temperature or motion, thereby introducing further components fields. These interactions contribute to the complexity of atmospheric behavior, and undoubtedly add to the difficulty of practical foreacasting.

The twelve-variable model just mentioned cannot picture the interactions between component fields having different wave lengths in the longitudinal direction, since it contains only one wave length. However, interactions among component fields having three different wave lengths are readily represented by a 28-variable model, which we shall presently introduce. In this study we propose to make an estimate of the range of practical predictability in the atmosphere, using the 28-variable model. The model will be formulated deterministically, so that two time-dependent solutions with identical initial conditions will be identical for all time. Thus the model will be perfectly predictable at all ranges when the initial conditions are known exactly. However, if the solutions are non-periodic, two or more solutions with nearly identical conditions should ultimately lose all resemblance to one another, and the time re-

quired for errors typical of observational errors in the real atmosphere to grow to errors which would be intolerable in the real atmosphere may be determined. The danger of basing the results upon unrepresentatively chosen initial conditions will be minimized by repeating the experiment many times.

2. The model

A simple model of the atmosphere which has already proven useful in reproducing certain features of thermally forced rotating flow is the geostrophic form of the two-layer model proposed by the writer (1960). In this model the stream functions for the nondivergent part of the flow in the two layers are denoted by $\psi + \tau$ and $\psi - \tau$, the potential temperatures in these layers by $\theta + \sigma$ and $\theta - \sigma$, and the individual pressure change at the surface separating the layers by ω. The model is most simply handled when horizontal variations of σ are excluded; it reduces essentially to one of the more familiar two-layer models, such as that of PHILLIPS (1951), when σ is treated as a pre-assigned constant.

In a recent paper, hereafter denoted by V, the writer (1963b) presented a general spectral form for the two-layer model without horizontal variations of σ. Here we shall summarize its principal features.

Let $F_0, F_1, \ldots$ denote a sequence of dimensionless functions of the horizontal space co-ordinates, satisfying the relations

$$\overline{F_i F_j} = \delta_{ij}, \tag{1}$$

$$\nabla^2 F_i = - L^{-2} a_i^2; F_i, \tag{2}$$

and the boundary conditions

$$\partial F_i / \partial s = 0, \tag{3}$$

where the bar denotes a horizontal average, L is a constant with the dimensions of distance, ∇^2 denotes a horizontal Laplacian operator, the quantities a_i are dimensionless constants, and $\partial / \partial s$ denotes a tangential derivative along the boundary. The dimensionless quantities

$$c_{ijk} = L^2 \overline{F_i J(F_j, F_k)}, \tag{4}$$

where J denotes a Jacobian with respect to the horizontal variables, then satisfy the relations

$$c_{ijk} = c_{ijk} = c_{kij} = -c_{ijk} = -c_{ikj} = -c_{kji}. \quad (5)$$

It is convenient to choose $F_0 = 1$, whence $a_0 = 0$, and $c_{0jk} = 0$ for all j and k.

An arbitrary function G of space and time may then be expanded in the series

$$G = S_G \sum_{i=0}^{\infty} G_i F_i, \quad (6)$$

where the coefficients G_i are functions of time alone, and the scale factor S_G has been chosen to make G_i dimensionless. Partial differential equations governing G may then be converted into ordinary differential equations governing G_i. In practice the sequence $F_0, F_1, \ldots$ is truncated, becoming the set $F_0, F_1, \ldots, F_N$, and all references to F_i and G_i, for $i > N$, are omitted in equations where they would ordinarily occur.

If scale factors $S_\psi = S_\tau = L^2 f$, $S_\theta = S_\sigma = BL^2 f$, and $S_\omega = f$ are chosen, where f is the Coriolis parameter, assumed constant, the prognostic equations of the spectral form of the model, according to V, simplify to

$$\dot{\psi_i} = \tfrac{1}{2} \sum_{j,k=1}^{N} a_i^{-2}(a_j^2 - a_k^2) \, c_{ijk}(\psi_j\psi_k + \tau_j\tau_k) + \psi_i^0, \quad (7)$$

$$\dot{\tau_i} = \tfrac{1}{2} \sum_{j,k=1}^{N} a_i^{-2}(a_j^2 - a_k^2) \, c_{ijk}(\psi_j\psi_k + \psi_j\psi_k) - a_i^2 \omega_i + \psi_i^0, \quad (8)$$

$$\dot{\theta_i} = \tfrac{1}{2} \sum_{j,k=1}^{N} c_{ijk}(\theta_j\psi_k - \psi_j\theta_k) + \sigma_0 \omega_i + \theta_j^0, \quad (9)$$

$$\dot{\sigma_0} = -\sum_{i=1}^{N} \theta_i \omega_i + \sigma_0^0 \quad (10)$$

while the thermal wind relation reduces to

$$\tau_i = \theta_i \quad \text{if} \quad a_i \neq 0. \quad (11)$$

Here B is a constant chosen to reduce to unity the factor of proportionality which would otherwise appear in (11), a dot denotes differentiation with respect to the dimensionless time ft, and ψ_i^0, τ_i^0, θ_i^0, and σ_0^0 denote the effects of friction and diabatic heating. An appropriate value for B is $8c_p^{-1}f$, where c_p is the specific heat of air at constant pressure.

In the present study, in the interests of simplicity, σ_0 is taken as a preassigned constant,

whereupon equation 10 is suppressed, and, according to equations (7)–(9), θ_0 is superfluous for the behavior of the remaining variables. As in V̇, the friction and heating are given by

$$\psi_i^0 = -k'\psi_i + k'\tau_i, \quad (12)$$

$$\tau_i^0 = k'\psi_i - (k' + 2k'')\tau_i \quad (13)$$

$$\theta_i^0 = -h\theta_i + h\theta_0^*, \quad (14)$$

where k' and k'' are dimensionless coefficients of friction at the lower surface and the surface separating the two layers, h is a coefficient of heating, and θ_i^* are constants defining a "thermal-equilibrium" temperature field, which would ultimately prevail if there were no motion.

Since τ is a stream function, the coefficient τ_0 is meaningless, while, in view of (11), τ_i may be replaced by θ_i for all other values of i. The variables ω_i may then be eliminated from equations (8) and (9), reducing them to a single prognostic equation (for each i).

Again as in V, the geometry is chosen to be that of an infinite channel of width πL. With x- and y-axes oriented along and across the channel, the fourteen functions

$$\phi_{0m} = \sqrt{2} \cos my/L; \quad m = 1, 2, \quad (15)$$

$$\phi_{nm} = 2 \sin my/L \cos nx/L;$$
$$m = 1, 2; \quad n = 1, 2, 3, \quad (16)$$

$$\phi'_{nm} = 2 \sin my/L \sin nx/L;$$
$$m = 1, 2; \quad n = 1, 2, 3, \quad (17)$$

are chosen as the set of orthogonal functions.

There are thus effectively 28 prognostic equations, governing the 14 variables ψ_i and the 14 variables θ_i. In addition to the 14 constant terms and 56 linear terms representing heating and friction, these 28 equations include a total 336 of nonlinear terms; 144 representing interactions between the zonal flow and the waves, and 192 representing interactions between waves of differing lengths. As mentioned in V, the number of waves about the circumference of the earth to be identified with a given wave length in a channel is not precisely defined, but it will be convenient to think of those waves for which $n = 1, 2$, and 3 as wave numbers 2, 4, and 6, respectively.

3. Properties of the model

In the solutions studied in V, all but one of the constants θ_l^* were set equal to zero; the remaining constant, the coefficient of the function ϕ_{01} in the expansion of the thermal-equilibrium temperature field, was denoted by θ_A^*, and served as a measure of the intensity of the thermal forcing. The coefficients k' and k'' were set equal respectively to h and $h/2$; since h had been made dimensionless through division by f, its reciprocal h^{-1} served as a measure of the speed of rotation. In the present model the constants have been similarly chosen.

It was found in V that different values of θ_A^* and h led to different regimes of flow. These included a Hadley regime, with no variations in the x-direction, a steady Rossby regime, in which waves moved uniformly without altering their shape, a vacillating Rossby regime, in which waves altered their shape in a regular periodic fashion, and a nonperiodic Rossby regime, in which the waves moved and altered their shape irregularly. It is to be anticipated that similar regimes will occur in the present model. Indeed, if all the coefficients associated with wave numbers 2 and 6 are initially zero, they will remain zero, and the equations governing the remaining variables, which represent the zonal flow and wave number 4, will reduce precisely to the equations appearing in V, Likewise, if wave numbers 2 and 4 are initially absent, they will not develop, and the zonal flow and wave number 6 will be governed by the same equations appearing in V.

Since the purpose of this study is to investigate atmospheric predictability, it is desirable that the solutions to be studied exhibit as much irregularity as that found in the atmosphere, if this is indeed possible. In view of the complexity of the present set of equations, suitable values of θ_A^* and h, as well as σ_0, which is preassigned, are best found by trial and error. Accordingly, we decided to choose values of θ_A^*, h, and σ_0 somewhat arbitrarily, and perform a sufficiently long integration to reveal the type of oscillation taking place. We planned to repeat this procedure, if necessary, until realistic oscillations were encountered.

Our first choice of constants led to periodic variations. Subsequent choices yielded irregular variations, with, however, a strong superposed two-day or three-day periodicity, which seemed

unrealistic. When an apparently suitable behavior was found with the values $\theta_A^* = 3/32$, $h = 5/32$, and $\sigma_0 = 5/128$, these values were chosen without further ado for detailed study. If all waves are absent initially, these values lead to the development of a Hadley circulation. This circulation proves to be stable with respect to wave number 2, but unstable with respect to wave numbers 4 and 6.

As already noted, if a disturbance of wave number 4 or 6 is now superposed upon this circulation, it must grow, and alter the zonal circulation, the ultimate result being a solution resembling one of those presented in V. If instead disturbances of both wave numbers 4 and 6 are superposed, it cannot be predicted in advance what will occur. Conceivably they could alter the zonal flow so that it would remain unstable with respect to only one wave, and the other wave would then dissapear. Alternatively, both waves could remain. Actually, for the chosen values of θ_A^*, h, and σ_0, the latter alternative occurs. Moreover, wave number 2 then develops. Evidently the ultimate maintenance of wave number 2, as well as the original development, is due to the interaction of wave numbers 4 and 6. These wave numbers are in turn maintained by the zonal field, which in turn is maintained by thermal forcing.

The first numerically obtained solution began with an initial state (which we shall call *state I*) consisting of the equilibrium Hadley circulation plus superposed small-amplitude disturbances of wave numbers 2 and 4. The reciprocal of the Coriolis parameter, assumed equivalent to 3 hours, was chosen as a time increment. The numerical integration was performed on the Facit-EDB electronic computer of the Norwegian Meteorological Institute in Oslo. The integration was allowed to run for a total of 512 iterations, or 64 days. The final state (which we shall call *state 0*) was assumed to be free of transient effects associated with unrepresentative initial conditions. That is, although state 0 was obviously determined by state I, having evolved from it, its features were assumed to be no more usual or unusual than those of a final state which would have evolved from some other arbitrarily chosen initial state. State 0 was then available as an initial state for further numerical solutions, which could be assumed to be representative throughout their history.

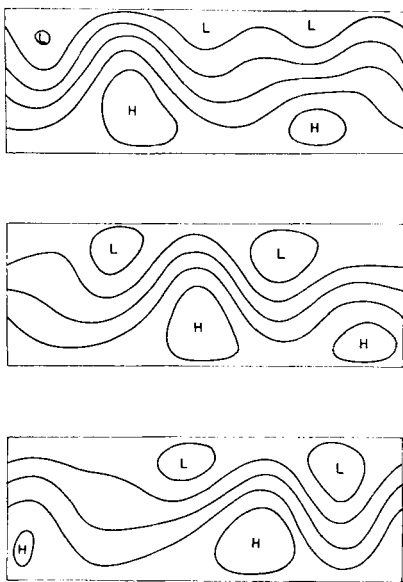Figure 1 shows three consecutive maps of the

FIG. 1. A sequence of stream function fields at the 500-millibar level, at intervals of one day, occurring in the numerical solution of the 28-variable model. The longitudinal extent shown is one complete wave length of the longest wave present.

field of ψ, at intervals of one day, beginning four days after state 0. The degree of resemblance to real atmospheric fields can readily be assessed. Although there is no provision for fine structure, the relative importance of wave numbers 2, 4, and 6 can vary from day to day. There is evidently a decrease in the dominant wave number at high latitudes, not accompanied by a similar decrease at low latitudes. Thus some of the irregular and rather unpredictable features of real atmospheric motion seem to have been captured.

4. The growth of small errors

The present section contains the principal results of this study. It concerns the growth-rate of errors superposed upon a basic solution, during such time as the errors may be regarded as being small. The chosen basic solution covers a time interval of $D = 64$ days, or 512 iterations, extending from an initial time t_0 to a final time t_D, and is obtained by choosing state 0 as the state at time t_0, and integrating the governing equations up to time t_D. It is convenient to designate the 28 variables ψ_i and θ_i by the new

names $x_1, ..., x_M$, where $M = 28$, the serial order of the variables being immaterial. The governing equations may then be written

$$\dot{x_i} = F_i(x_1, ..., x_M); \quad i = 1, ..., M, \quad (18)$$

and the basic solution, beginning with state 0 at time t_0, may be written

$$x_i = Z_i(t) \quad \text{for} \quad t_0 \leqslant t \leqslant t_D. \quad (19)$$

The basic solution is determined explicitly by numerical integration.

If $\quad x_i = Z_i(t) + y_i(t) \quad (20)$

represents an additional solution of equations (18), and if the components y_i of the error, or the difference between this solution and the basic solution, are small, the errors y_i are approximately governed by the linear equations

$$\dot{y_i} = \sum_{j=1}^{M} \frac{\partial F_i}{\partial x_j} y_j, \quad (21)$$

in which the coefficients $\partial F_i / \partial x_j$ are time-dependent. Equations (21) possess the solution

$$y_i(t'') = \sum_{j=1}^{M} a_{ij}(t'', t') \, y_j(t'), \quad (22)$$

or, in matrix form

$$Y(t'') = A(t'', t') \, Y(t'), \quad (23)$$

where Y is a matrix of M rows and one column and A is a matrix of M rows and M columns, whose elements depend upon the basic solution $Z_i(t)$ during the interval $t' \leqslant t \leqslant t''$. The matrix A controls the growth of small errors during this interval, and will be called an *error matrix*. It is evident that for any three times t', t'', t''',

$$A(t''', t') = A(t''', t'') A(t'', t'). \quad (24)$$

For any two times t', t'' the error matrix $A(t'', t')$ is most readily determined numerically. Choosing a new state x_i at time t' which differs from the basic solution $Z_i(t')$ in only one component, say

$$y_i(t') = \varepsilon \delta_{iK}, \quad (25)$$

where ε is small, we find from (22) that

$$y_i(t'') = \varepsilon a_{iK}(t'', t'). \quad (26)$$

Thus, when the basic solution is subtracted from the new solution at time t'', the result is ε times the Kth column of $A(t'', t')$. Repeating this procedure M times, for the M different values of K, we may obtain the matrix $A(t'', t')$.

This entire procedure was performed 32 times, with $t' = t_0, t_2, ..., t_{62}$, and with t'' in each case exceeding t' by 2 days, the subscripts denoting the number of days, or one eight the number of iterations, following state 0. This procedure yielded the 32 error matrices $A(t_{i+2}, t_i)$, for $i = 0, 2, ..., 62$.

These matrices were then multiplied together in pairs, yielding, in view of (24), the 16 error matrices $A(t_{i+4}, t_i)$, for $i = 0, 4, ..., 60$. Further matrix multiplication yielded eight matrices $A(t_{i+8}, t_i)$, four matrices $A(t_{i+16}, t_i)$, two matrices $A(t_{i+32}, t_i)$, and finally the single matrix $A(t_{64}, t_0)$. Thus there were available sets of error matrices controlling the growth of small errors during 2-day, 4-day, 8-day, 16-day, 32-day, and 64-day periods.

It is convenient to treat an individual set of errors y_i as a point in a 28-dimensional phase space whose coordinates are $y_1, ..., y_M$. By the *amplitude* of the error we shall mean the distance of this point from the origin. An ensemble of initial errors, each of amplitude ε, but random in that no direction in 28-dimensional space is preferred over any other direction, then occupies the surface of the 28-dimensional sphere

$$\sum_{i=1}^{M} y_i^2(t') = \varepsilon^2 \qquad (27)$$

or, in matrix form

$$Y^T Y = \varepsilon^2, \qquad (28)$$

where the superscript T denotes the transpose of a matrix. If each error in the ensemble is allowed to evolve according to equation (23), the sphere will be deformed into the ellipsoid

$$Y^T (AA^T)^{-1} Y = \varepsilon^2 \qquad (29)$$

at time t''.

The matrix AA^T possesses M real non-negative eigenvalues. If these are denoted by $\lambda_1^2, ..., \lambda_M^2$, the lengths of the semiaxes of the ellipsoid are $\varepsilon\lambda_1, ..., \varepsilon\lambda_M$. Since the sum of the eigenvalues of a matrix equals the trace, or diagonal sum,

$$\sum_{i=1}^{M} \lambda_i^2 = \sum_{i,j=1}^{M} a_{ij}^2. \qquad (30)$$

At time t'' the squared-amplitude of an arbitrary error whose initial squared-amplitude was ε^2 will be

$$\sum_{i=1}^{M} y_i^2(t'') = \sum_{i,j,k=1}^{M} a_{ij} a_{ik} y_j(t') y_k(t). \qquad (31)$$

If square brackets [ ] denote an ensemble average, the ensemble mean-square error at time t' is obviously

$$\left[\sum_{i=1}^{M} y_i^2(t')\right] = \varepsilon^2 \qquad (32)$$

in view of (27), while at time t'' it will be

$$\left[\sum_{i=1}^{M} y_i^2(t'')\right] = \sum_{i,j,k=1}^{M} a_{ij} a_{ik} [y_j(t') y_k(t')]. \qquad (33)$$

Because of the randomness of the ensemble, the factor in brackets on the right of (33) vanishes if $j \neq k$, and reduces to ε^2/M if $j = k$. It follows from (30) the that

$$\left[\sum_{i=1}^{M} y_i^2(t'')\right] = M^{-1} \sum_{i=1}^{M} \lambda_i^2 \varepsilon^2, \qquad (34)$$

i.e., the mean-square amplitude at time t'' is the mean-square length of the axes of the ellipsoid, and the amplification $\alpha(t'', t')$ of the root-mean-square error, between times t' and t'' is

$$\alpha(t'', t') = \left(M^{-1} \sum_{i=1}^{M} \lambda_i^2\right)^{-\frac{1}{2}}. \qquad (35)$$

Accordingly, for each of the 32 error matrices $A(t_{i+2}, t_i)$, the amplification $\alpha(t_{i+2}, t_i)$ was determined. These values, arranged in chronological order, give a history of the growth-rate of small initially random errors during successive two-day periods.

Since an error which is random at time t_i will grow to a nonrandom error by the time t_{i+2}, the amplification of initially random errors during a four-day period is not the product of the amplifications of initially random errors during two consecutive two-day periods. Accordingly, amplifications $\alpha(t_{i+4}, t_i)$ for the 16 four-day periods were determined directly from the 16 matrices $A(t_{i+4}, t_i)$. Likewise, the eight amplifications $\alpha(t_{i+8}, t_i)$, four amplifications $\alpha(t_{i+16}, t_i)$, two amplifications $\alpha(t_{i+32}, t_i)$, and the single amplification $\alpha(t_{64}, t_0)$ were evaluated from the corresponding matrices.

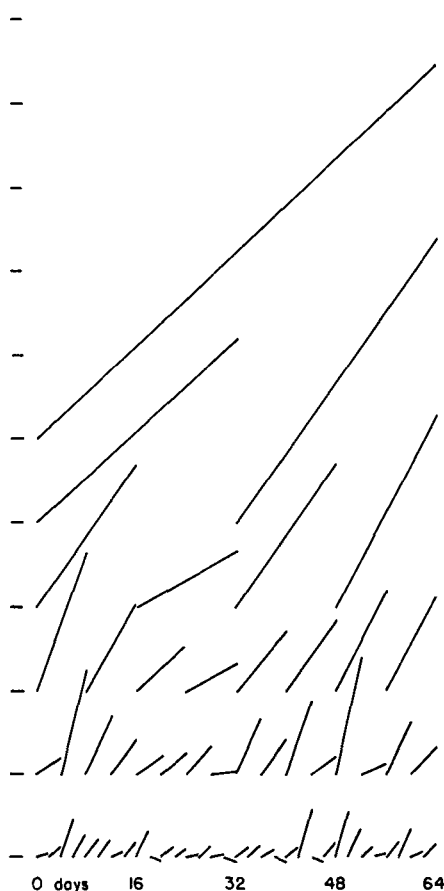In Fig. 2, which presents the principal results

FIG. 2. *Amplifications of initially random errors.* Projection of segment on vertical scale at left indicates total amplification during period indicated by horizontal projection of segment. Scale marks on vertical scale are separated by factors of ten.

of this section, each line segment depicts the behavior, during a specific time interval, of errors which were random at the beginning of the interval. The projection of the segment on the time scale at the base of the figure locates the interval, while the length of the vertical projection indicates the amount of amplification. The slope of the segment therefore indicates the rate of amplification; the scales have been chosen so that a forty-five-degree slope corresponds to a four-day doubling time. The use of straight line segments is not intended to imply that the growth rate within any interval is uniform.

Perhaps the most striking feature is the great

variability of the growth rates during the 64 days under study. There were four 2-day periods during which random errors actually diminished, while during others they increased by a factor of three or more. During one 8-day period small random errors grew less than threefold, while during another they grew more than fortyfold. The amplification is therefore not an atmospheric constant, but depends strongly upon the circulation pattern.

Three intervals occurred, one near the beginning of the 64-day period, and two during the latter half, when the growth-rate might be considered explosive. The maps shown in Fig. 1 occurred during the first of these intervals. A brief inspection failed to reveal any obvious prominent feature which distinguished the circulation patterns at these times from those during the remainder of the 64 days. There must of course have been some rather complicated functions of the circulation pattern which were abnormal at these times, since the amplification itself is a function of the circulation.

What, then, can be said about the maximum range of acceptable forecasts, if by forecasts we mean forecasts of the complete state of the atmosphere at specific times? Such a range depends upon the maximum allowable growth of initial errors. Over areas such as Europe and North America, where observations are dense and map analyses are fairly accurate, an initial error might grow by a factor of ten or more before becoming intolerable. Over regions of scanty data, such as much of the Pacific Ocean, it is questionable whether even a factor of two can be tolerated. For the globe as a whole, one might say that initial errors have grown to intolerable errors when they have amplified by a factor of five.

Fig. 2 reveals one 16-day period, out of a total of four, when small errors grew only fivefold. At the beginning of this period, an acceptable two-week forecast could have been made. Fig. 2 also shows three four-day periods, out of a total of sixteen, when small errors grew at least sevenfold. At the beginning of these periods, acceptable forecasts would have been limited to three days.

On the strength of the 28-variable model, it therefore appears that during a fair portion of the time extended-range forecasts, or, specifically, forecasts a week or more in advance, are feasible. This range extends beyond the range

at which successful forecasts of instantaneous states of the atmosphere are now generally made operationally. On the other hand, the model offers little promise for forecasting instantaneous states a month in advance.

Of course there is no assurance that the time-scale in the model is realistic. There are various reasons why developments requiring a certain time in the model may require a different time in the real atmosphere. For one thing, the chosen value $\theta_A^* = 3/32$ corresponds to an equator-to-pole contrast of 155°C in the equilibrium temperature field at 500 millibars, or an average contrast of about 100°C in the existing temperature field, which is time-variable. The corresponding average zonal wind speed at 500 millibars in middle latitudes is about 50 meters per second. These values would be more realistic if diminished by a factor of two.

If both θ_A^* and h are diminished by the same factor, and if the initial values of $x_1, ..., x_M$ are decreased by this factor, the development of the system with time will likewise be slowed down by this factor, but will otherwise be unchanged. Thus it may be reasonable to conclude that the time required for typical errors to become intolerable ranges from about a week to about a month, rather than the smaller values already cited.

On the other hand, the model is devoid of small-scale features, which typically fluctuate with short periods, and should contribute toward a more rapid decay of predictability than that occurring in the model. Despite these considerations, it is hoped that the model will afford a fair assessment of the ultimate possibilities of extended-range prediction, until such time as further experiments with more detailed models may be performed.

5. The nonlinear phase of growth

The foregoing section has dealt with the growth of errors during such time as they may be considered small. Since the errors continue to grow while they are still small, they must eventually cease to be small, whereupon the linearized equations governing them will no longer hold. The errors have then entered the nonlinear phase of growth. During this phase the growth rate must eventually subside, since ultimately the errors will become only as large

as the difference between two randomly chosen states of the system. Whether or not long-range forecasting, or forecasting at any range beyond the linear phase of growth, is a feasible task depends upon the behavior of errors during the nonlinear phase.

It is common experience that in the real atmosphere the locations and intensities of cyclones and anticyclones and features of larger scale can be predicted with reasonable accuracy at ranges at which the locations and intensities of individual thunderstorms and other small-scale features cannot be predicted. It would seem that errors in small-scale features enter their own nonlinear phase of growth, and perhaps reach their ultimate size, while errors in the large-scale features are still in the linear phase.

The question is frequently asked as to whether there are certain large-scale features of the atmosphere which can be predicted at a range at which other large-scale or cyclone-scale features are no longer predictable, just as cyclones are predictable at a range at which thunderstorms are no longer predictable. Many currently practiced methods of long-range forecasting are based upon the assumption that this question may be answered affirmatively; by and large there is no attempt to forecast such details as locations of individual cyclones several weeks or longer in advance.

Models such as the 28 variable model might seem to be suitable for answering questions like the one just posed. Unfortunately, however, treatment as systematic as our treatment of the linear phase of growth does not appear feasible. There is a virtually unlimited number of nonlinear functions of the 28 variables which conceivably might have the property of long-range predictability. The labor involved in testing a large number of such functions would be prohibitive, even with so simple a model.

Accordingly, we shall simply discuss the behavior of one particular nonlinear function of the variables, which has appeared upon inspection to possess some predictability at extended ranges. This quantity is the quadratic function

$$Q = \psi_{21}\psi_{22} + \psi_{21}'\psi_{22}', \qquad (36)$$

where ψ_{21}, ψ_{22}, ψ_{21}', and ψ_{22}' are four of the 28 variables $x_1, ..., x_M$, namely the coefficients of the orthogonal functions ϕ_{21}, ϕ_{22}, ϕ_{21}', ϕ_{22}', as
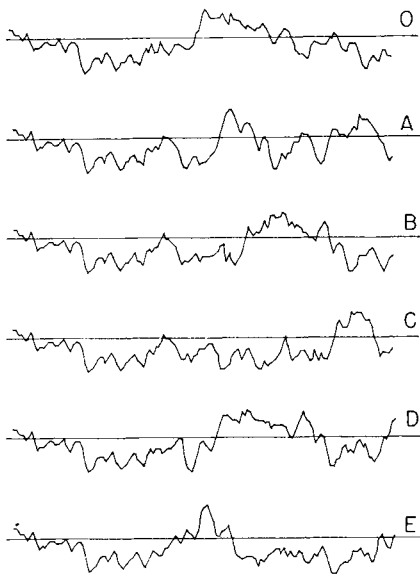
FIG. 3. Behavior of Q during a 128-day period. The six curves are for numerical solutions with slightly different initial conditions. Horizontal lines are zero lines.

defined by expressions (16) and (17), in the expansion (6) of the field of ψ.

This quantity assumes positive values when wave number 4 in the field of ψ possesses a large amplitude in low latitudes and a small amplitude in high latitudes, while it assumes negative values when the opposite situation occurs. In the maps in Fig. 1, Q is not far from zero. Because of symmetries in the governing equations (7)–(10), the long-term average value of Q should be zero, unless the system is intransitive—i.e., unless there are two distinct regimes, one characterized by a positive and one by a negative average value of Q, such that whichever regime first becomes established as a result of the chosen initial conditions will persist forever.

Fig. 3 presents six curves for the behavior of Q during a 128-day period. In curve 0, the initial state is state 0, while in the remaining curves the initial states are very small departures from state 0. The initial errors were chosen so small that the linear phase lasts about 48 days. Beyond this time there is no single preferred course of behavior. Thus the detailed behavior of Q does not seem to be predictable at long range.

By contrast, Fig. 4 shows the behavior of Q during a single 768-day period, beginning with state 0. For convenience in presentation, the period is divided into six consecutive segments. Beyond the evident lack of periodicity, the most outstanding feature is the occurrence of extended intervals, sometimes as long as four months, in which Q possesses the same sign. Thus Q is a highly persistent quantity.

It follows that one can forecast the sign of Q a number of weeks in advance simply by predicting that the sign will be the same as at present. Such a forecast is by no means certain to succeed, but statistically it has a higher probability of succeeding than of failing. In contrast to the extreme accuracy of initial conditions required for extended forecasts of the detailed behavior of Q, the errors in observing the initial values of the 28 variables may be fairly large without disturbing the forecast of the sign of Q, provided that they are not so large as to yield the wrong initial sign for Q. Hence the envisioned forecast should extend well into the nonlinear phase.

These results seem to agree with experience in predicting the behavior of the real atmosphere. Little success has been obtained in predicting detailed instantaneous states at long range, but numerous statistical formulas, in
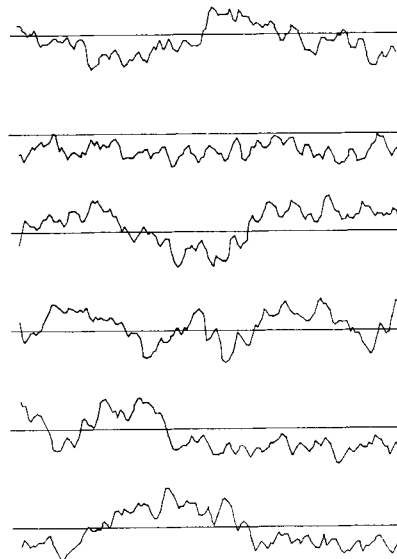

FIG. 4. Behavior of Q during a 768-day period. The six curves are successive segments of the same numerical solution. Horizontal lines are zero lines.

TABLE 1. *Square roots* $\lambda_1, ..., \lambda_7$ *of seven largest eigenvalues of matrices* $A(t_{i+4}, t_i)A^T(t_{i+4}, t_i)$, *for 16 successive 4-day periods.*

i	λ_1	λ_2	λ_3	λ_4	λ_5	λ_6	λ_7
0	6.3	4.2	2.9	1.3	1.3	0.9	0.4
4	93.8	2.5	1.5	0.9	0.6	0.4	0.1
8	25.1	5.3	3.9	2.3	1.1	0.7	0.5
12	10.0	7.0	4.9	2.6	1.6	1.3	0.8
16	7.1	3.1	1.8	1.3	0.8	1.0	0.2
20	7.2	4.9	3.7	2.4	1.3	0.7	0.6
24	8.5	4.5	3.9	3.0	2.0	1.2	0.5
28	3.7	2.5	2.1	1.8	1.2	1.0	0.6
32	10.8	7.6	6.5	3.3	1.6	1.2	0.7
36	7.1	3.7	2.1	1.8	1.6	1.3	0.6
40	38.5	7.4	5.1	2.0	1.0	0.6	0.5
44	6.7	4.3	0.2	1.2	1.0	0.8	0.4
48	126.3	2.5	2.2	0.9	0.6	0.4	0.1
52	5.4	2.9	2.4	1.8	1.3	1.0	0.6
56	16.4	11.0	9.1	6.1	3.7	0.9	0.7
60	8.0	5.6	3.8	2.5	1.2	1.1	0.7

some cases linear, have seemed to yield positive reductions of variance.

It should also be noted that the model allows for no long-term interaction of the atmosphere with its environment. The persistence of Q arises in this case entirely from internal dynamics.

In passing it is worth noting that the mean value of Q in Fig. 4 is decidedly negative, suggesting that the system may be intransitive. However, continuation of the integration for an additional year beyond the interval shown in Fig. 4 yielded a preponderance of positive values. Evidently even in so simple a model two years of data form an insufficient sample for reliable climatological estimates.

6. Further considerations and conclusions

The foregoing sections have shown that if a system is evolving with time in accordance with the model equations, small random errors in observation will grow until they become significant features of the total field of motion. Although the growth rate of these errors is extremely variable, errors comparable to those currently made in observing the real atmosphere always seem to grow to intolerable errors in less than a month, and occasionally in less than a week. Before any similar statement is made concerning the behavior of the real atmosphere, it would be highly desirable to

TABLE 2. *Square roots* $\lambda_1, ..., \lambda_7$ *of seven largest eigenvalues of matrices* $A(t_{i+8}, t_i)A^T(t_{i+8}, t_i)$, *for 8 successive 8-day periods.*

i	λ_1	λ_2	λ_3	λ_4	λ_5	λ_6	λ_7
0	242.1	5.1	3.1	0.7	0.4	0.2	0.0
8	50.8	14.8	6.9	2.7	1.0	0.7	0.3
16	16.5	5.0	3.9	1.9	1.0	0.4	0.0
24	9.2	4.4	3.4	2.9	2.3	1.2	0.0
32	24.8	11.3	7.5	2.9	1.1	1.1	0.2
40	36.3	10.7	4.5	1.8	2.7	0.6	0.0
48	86.8	2.9	1.7	1.2	0.7	0.4	0.0
56	55.9	38.0	15.4	5.8	1.9	0.9	0.4

perform similar studies, using systems of equations whose solutions afford much better simulations of real atmospheric behavior.

The previously mentioned model of SMAGORINSKY (1963) possesses 5184 variables, as opposed to the 28 variables of our model. It is immediately obvious that the procedure of this study could not feasibly be repeated with a model as large as Smagorinsky's; the performance of 5184 separate numerical integrations, each with a set of initial conditions differing from a basic set in only one variable, would be absolutely prohibitive with current computers and with any envisioned in the near future.

A possible modification would be to use not 5184 sets of initial conditions but some small number, perhaps 10 or 20, chosen in some random fashion. A study of the growth rate of errors for these cases might yield much of the desired information. The following considerations, based upon the 28-variable model, are in order.

In 28-dimensional phase space, a small sphere representing an ensemble of initial states becomes deformed into an ellipsoid. The mean-square distance from the center of the ellipsoid, given by the mean eigenvalue of the matrix $\varepsilon^2 A A^T$, where A is the error matrix, eventually becomes very large, but, as a result of the dissipative terms in the governing equations, the square of the volume of the ellipsoid, given by the product of the eigenvalues of $\varepsilon^2 A A^T$, shrinks toward zero. It follows that some of the eigenvalues of $A A^T$ become much larger than others, i.e., the ellipsoid becomes extremely elongated in a few directions.

Table 1 lists the square roots of the largest seven eigenvalues of the sixteen matrices $A(t_{i+4}, t_i) A^T(t_{i+4}, t_i)$. These quantities represent the lengths of the seven longest semi-axes of the ellipsoids, which, four days earlier, were spheres of unit radius. There is considerable variation from one four-day period to another; however, there are invariably at least three, and never more than six, semi-axes longer than the radius of the original sphere. In some instances the longest axis is far longer than the second-longest.

Table 2 is similar to table 1, except that it refers to the eight matrices $A(t_{i+8}, t_i) A^T(t_{i+8}, t_i)$. The same features are evident, and the tendency for the largest eigenvalue to dominate is even stronger.

It follows that after eight days there will be a strong tendency for a randomly chosen point on the ellipsoid to be displaced from the center in a direction nearly parallel to the longest axis. In other words, even though the initial error field may be completely unknown, the general configuration of the error field after eight days can be reasonably well estimated, although the sign will of course be in doubt. It need hardly be added that there are occasions when such knowledge would be of practical importance.

It also follows that after a few days the growth rate of initially random errors is strongly influenced by the growth of the largest single eigenvalue. This growth rate may be estimated moderately well by considering a single initial error field, and even more closely from studying perhaps four or five initial error fields.

If more realistic models with many thousand variables also have the property that a few of the eigenvalues of the many-thousandth-order matrices $A A^T$ are much larger than the remaining eigenvalues, a study based upon a small ensemble of initial errors should, as already suggested, give a reasonable estimate of the growth rate of random errors. Moreover, it may even indicate, apart from sign, certain preferred configurations of the error field. It would appear, then, that best use could be made of computation time by choosing only a small number of error fields for superposition upon a particular initial state, thus hopefully allowing the study of perturbations upon a considerable number of different initial states.

Acknowledgments

REFERENCES

LORENZ, E. N., 1960, Energy and numerical weather prediction. *Tellus*, 12, pp. 364–373.

LORENZ, E. N., 1962, The statistical prediction of solutions of dynamic equations. *Proc. Internat. Sympos. Numerical Weather Prediction*, Tokyo, Japan, pp. 629–635.

LORENZ, E. N., 1963a, The predictability of hydrodynamic flow. *Trans. New York Acad. Sci.*, Ser. 2, 25, pp. 409–432.

LORENZ, E. N., 1963b, The mechanics of vacillation. *J. Atmos. Sci.*, 20, pp. 448–464.

PHILLIPS, N. A., 1951, A simple three-dimensional model for the study of large-scale extratropical flow patterns. *J. Meteor.*, 8, pp. 381–394.

PHILLIPS, N. A., 1956, The general circulation of the atmosphere: a numerical experiment. *Q.J. Roy. Meteor. Soc.*, 82, pp. 123–164.

SMAGORINSKY, J., 1963, General circulation experiments with the primitive equations. I. The basic experiment. *Mon. Weather Rev.*, 91, pp. 99–164.

THOMPSON, P. D., 1957, Uncertainty of initial state as a factor in the predictability of large scale atmospheric flow patterns. *Tellus*, 9, pp. 275–295.